Applied Surface Science, Volume 256, Issue 15, 15 May 2010, Pages 4771-4776

Accepted Manuscript



Title: Defects of SiC nanowires studied by STM and STS

Authors: A. Busiakiewicz, A. Huczko, T. Dudziak, M. Puchalski, W. Kozłowski, M. Cichomski, Z. Klusek, W. Olejniczak

PII: S0169-4332(10)00140-6
DOI: doi:10.1016/j.apsusc.2010.01.102
Reference: APSUSC 19791

To appear in: *APSUSC*

Received date: 15-9-2009
Accepted date: 19-1-2010

Please cite this article as: A. Busiakiewicz, A. Huczko, T. Dudziak, M. Puchalski, W. Kozłowski, M. Cichomski, Z. Klusek, W. Olejniczak, Defects of SiC nanowires studied by STM and STS, *Applied Surface Science* (2008), doi:10.1016/j.apsusc.2010.01.102

This is a PDF file of an unedited manuscript that has been accepted for publication. As a service to our customers we are providing this early version of the manuscript. The manuscript will undergo copyediting, typesetting, and review of the resulting proof before it is published in its final form. Please note that during the production process errors may be discovered which could affect the content, and all legal disclaimers that apply to the journal pertain.

ACCEPTED MANUSCRIPT

Defects of SiC nanowires studied by STM and STS

A. Busiakiewicz[1,*], A. Huczko[2], T. Dudziak[3], M. Puchalski[1], W. Kozłowski[1], M. Cichomski[4], Z. Klusek[1], W. Olejniczak[1]

[1] Department of Solid State Physics, Division of Physics and Technology of Nanometer Structures, University of Łódź, Pomorska 149/153, 90-236 Łódź, Poland

[2] Department of Chemistry, Warsaw University, Pasteura 1, 02-093 Warsaw, Poland

[3] Cranfield University, Power Generation Technology Centre, Cranfield, Bedfordshire MK43 0AL, U.K.

[4] Department of Chemical Technology and Environmental Protection, University of Łódź, Pomorska 163, 90-236 Łódź, Poland

Abstract

For the first time the scanning tunneling microscopy (STM) and scanning tunneling spectroscopy (STS) are employed to investigate the morphology and the surface electronic structure of the defective silicon carbide nanowires (SiCNWs). The SiCNWs produced via combustion synthesis route are studied. The STS measurements are performed in the current imaging tunneling spectroscopy mode (CITS) that allows us to determine the correlation between STM topography and the local density of electronic states (LDOS) around the bend of an isolated SiCNW. The measurements reveal fluctuations of LDOS in the vicinity of the defect. The local graphitization and the inhomogeneous concentration of doping impurities (e.g. nitrogen, oxygen) are considered to explain these fluctuations of metallic-like LDOS in the vicinity of the SiCNW's deformation.

Keywords: Silicon carbide, Nanowire, Defect, STM, STS

*Corresponding author: Adam Busiakiewicz
Tel.: +48 42 6355694
Fax.: +48 42 6350030
E-mail: adambus@std2.phys.uni.lodz.pl

Accepted Manuscript

ACCEPTED MANUSCRIPT

1. Introduction

Because of its outstanding physical properties, silicon carbide (SiC) is a very promising material for high power, high temperature and high frequency applications [1,2]. In recent years, SiC has been also found to form various one-dimensional (1-D) nanostructures (e.g. nanowires and nanotubes) and this fact makes SiC attractive for construction of nanoelectronic devices like SiCNW-based transistor [3]. SiC-based 1-D nanostructures have been synthesized using many different processes (see [4,5] and references therein). Recently, it has been demonstrated that SiC nanowires (SiCNWs) can be produced also via thermolysis-induced carbonization of halocarbons (combustion synthesis) which is efficient single step chemical reaction performed in a closed reactor without external heating of the reactants [6].

The ideal SiCNWs are generally thin elongated SiC nanocrystals. However, SiCNWs usually possess various structural defects that can be divided into two classes: (i) 'large-scale' deformations (e.g. diameter fluctuations [7], Y-junctions [8], bends [9], springs [10] or "S"-shaped sections [11]) and (ii) 'atomic-scale' defects (e.g. vacancies and antisites [12] or interstitials [13]). In general, the first class of defects is characteristic of all 1-D nanostructures (e.g. like in the case of carbon nanotubes [14]) and the second class is related to the specific crystallographic properties of SiC material. These two families of defects are of course in close relationship because the deformation of SiCNW must be accompanied by the existence of defects at atomic level. Furthermore, it is widely known that the atomic-scale defects perturb the local electronic structure of bulk SiC crystals [15-18]. In this context it is reasonable to expect that the defects influence the local surface electronic structure of SiCNWs as well. The electronic structure of the cubic 3C-SiC crystal can be altered by the existence of unintentionally introduced nitrogen dopant [19].

Accepted Manuscript

ACCEPTED MANUSCRIPT

Similarly, the band structure of 1-D SiC nanostrutures (nanotubes [20] and nanowires [21,22]) can be affected by nitrogen. It is also shown that electronic structure of SiCNWs can be modified when their surface is passivated with hydrogen [23]. Due to these facts, the local contamination and doping of the defected SiCNW's region should be also taken into account to explain local LDOS fluctuations. The present knowledge about defects and deformations of SiCNWs is very limited. However, this knowledge is necessary for understanding and designing the future SiCNWs-based nanoelectronic devices.

The aim of this study is to explore, for the first time, the fluctuations of the local density of electronic states (LDOS) in the vicinity of a SiCNW's deformation. Scanning tunneling microscopy (STM) and scanning tunneling spectroscopy (STS) are applied to reveal the topography and the local electronic structure of a bended SiCNW. STS is used in the current imaging tunneling spectroscopy (CITS) mode which allows us to correlate STM images with the surface LDOS distribution. We believe that these experiments provide new information about the surface electronic properties of defective SiCNWs.

2. Experimental

The STM/STS/CITS experiments are performed with a commercial VT-STM/AFM system in UHV conditions (Omicron GmbH, Germany). The concentration of SiCNWs on the samples is determined by using scanning electron microscope (SEM) Quanta 200 FEI. The STM tips are prepared by cutting 90%Pt-10%Ir alloy wires (Goodfellow) mechanically. Silicon carbide nanowires are produced by the thermolysis-induced carbonisation of halocarbons (combustion synthesis) [6]. The initial reactant composition comprises of polytetrafluoroethylene

Accepted Manuscript

ACCEPTED MANUSCRIPT

(PTFE, 57.8 wt%) and calcium disilicide ($CaSi_2$, 42.2 wt%) which gives the highest SiC yield. The obtained product is purified by calcination in air (900K, 1h) and a subsequent washing with KOH (30 wt%), H_2SO_4 (96 wt%) and HCl (36 wt%). Washing the material in distilled water and drying follow each stage of purification. A piece of the purified product is then diluted in 1,2-dichloroethane using the ultrasonic treatment (about 15 min). In the last step, we put a droplet of the mixture on the highly orientated pyrolytic graphite (HOPG) substrate and leave the sample to dry up. After that the sample is transferred into the UHV system and investigated without further preparation.

In the CITS mode, the I/V curves (128 points per single curve) are recorded simultaneously with a constant current image (256 points × 256 points) by the use of an interrupted-feedback-loop technique. Based on these measurements, the first derivative of the tunneling current with respect to the voltage (dI/dV) is calculated. The dI/dV spectra are normalized by dividing the differential conductance by the total conductance to obtain (dI/dV)/(I/V) [24]. The divergence problem in this case is overcome by applying some amount of broadening (ΔV) to the I/V values [25] (ΔV=1 V for all curves in our case). Topographic STM images are collected in the constant current mode at the positive sample bias voltage U_s=0.2-1 V and the tunneling current set point I=0.2-1.0 nA.

3. Results and discussion

The distribution of the SiCNWs is preliminarily determined by using SEM and a representative image (secondary electrons detector) is shown in Fig. 1. In the upper part of the image, a relatively large concentration of SiCNWs can be observed. Such a concentration and a tangle of SiCNWs is not suitable for STM measurements because

Accepted Manuscript

ACCEPTED MANUSCRIPT

of the high probability of the STM tip damage. In the central part of the imag,e a bunch of SiCNWs is also visible. The typical diameter of the SiCNWs is estimated to be in the range of 10-100 nm. The SiCNWs' length usually exceeds 1 μm but it can also be as large as several tens of μm. Most of the observed SiCNWs are straight but some objects exhibit the existence of deformations. In the lower part of the area (especially in the right down corner), the concentration of SiCNWs is relatively small and objects lie flat on the substrate which opens the possibility for STM measurements of individual and isolated objects and their defects.

The topographic STM image of a bended SiCNW is presented in Fig. 2a. The maximum height of the object on both sides of the bend is in the range of 96-100 nm relative to the HOPG substrate. This almost constant value of the relative height over the whole deformation region suggests that the bended nanowire is lying almost flat on the substrate and this is confirmed by an excellent stability of the object during STM/STS investigations. Furthermore, it can also be supposed that this high stability is the fingerprint of good electrical contact between the substrate and the nanowire due to the strong interaction between them. The width of the nanowire in plane of the sample is about 400-450 nm which is approximately 4 times more than the observed height. It is quite probable that the tip convolution effect should be here taken into account [26] to explain this discrepancy. However, it is also possible that the nanowire consists of a few thinner nanowires (we have reported a similar effect previously [27]), forming a kind of flattened bundle. The angle between the two parts of the bended nanowire is 126º±2º. The more detailed image of the SiCNW's deformation is presented in Fig. 2b where we apply the standard deviation filter to expose existing edges. We can see that there are shallow trenches, less than 5 nm deep, running along the nanowire. In the deformation region, we can observe more

Accepted Manuscript

ACCEPTED MANUSCRIPT

complicated structures. From Fig. 2a and 2b it is clear that some parts of the nanowire are completely broken and sharp edges of these broken parts are exposed in the region of deformation (denoted by white arrows in Fig. 1a). Because the SiCNWs produced in combustion synthesis are mostly 3C-SiC nanowires, and they are predominantly with [111] orientation (see [6]), it is probable that this deformation resembles the geometry of large-diameter nanowire under mechanical bending [9]. In this context we suppose that the deformation was rather formed after the synthesis process (e.g. during purification, ultrasonic treatment, or deposition). However, we think that the violent nature of combustion synthesis also allows formation of such defects.

To investigate the surface electronic properties of the SiCNW in the vicinity of the bend, we apply the STS technique. The typical behaviour of the I(V) spectroscopic curves (averaged by 10 points × 10 points) is presented in Fig. 3. Two curves represent the area on the left (I) and on the right (II) outside the bend of the SiCNW (dashed and dash-dotted grey line, respectively). It is clear that these curves have very similar shape, i.e. they are asymmetric with respect to 0 V because the absolute current values are smaller for negative sample bias voltages than for the positive sample bias voltages. It means that surface electronic properties on both sides of SiCNW outside the deformation are similar. These I(V) traces show no existence of the band gap (~2.2 eV for bulk 3C-SiC) and are similar to the I(V) traces recorded previously for SiCNWs deposited on gold substrate. As we proposed previously [21], the shape of those I(V) curves can be attributed to n-type semiconducting properties of nitrogen-doped SiCNW's surface, or alternatively, to the surface carbon enrichment. It should be admitted here that the reproducibility of I(V) curves on gold (previous study [21]) and HOPG (this study) also suggests that the type of the substrate, i.e. gold or HOPG, does not affect the I(V) measurements substantially. In

Accepted Manuscript

ACCEPTED MANUSCRIPT

the case of the I(V) curve representing the deformation region (III, solid black line), one can notice increased absolute values of the current at negative biases which means that the I(V) curve becomes more symmetric. For comparison, the I(V) trace recorded on bare HOPG substrate is shown (dotted black line). This is almost symmetric which is characteristic of flat terraces of the semimetallic HOPG surface in the STS low voltage limit (below 1 V) [28]. In this context we suggest that the evolution of the I(V) shape from asymmetric (far from deformation) to more symmetric shape (close to deformation) may be ascribed to the change of the SiCNW's chemical composition near the deformation. Although it was proposed that mechanical bending weakly influences the atomic coordination near the deformation [9], it seems to be probable that the chemical composition can be changed by the diffusion of atomic scale defects, like Si and C interstitials, that can migrate and tend to agglomerate in the vicinity of deformations at elevated temperatures. Furthermore, it should be noted that the activation temperatures are different for C (450 K) and Si (650 K) interstitials [29]. Because the activation temperature is lower for C interstitials, it suggests their higher mobility at elevated temperatures. Thus, we think that in our case the calcination of SiCNWs performed at 900 K can be responsible for the privileged segregation of C interstitials when a locally graphitised region is formed in the vicinity of SiCNW's deformation. However, the comparison of the I(V) traces recorded over the bend and bare HOPG shows that they are not identical. This can be attributed to only partial graphitisation of SiC and forming a carbon-enriched subsurface region which has electronic properties halfway between SiC and graphite.

The calculated first derivative dI/dV and (dI/dV)/(I/V) curves for different regions of the SiCNW are presented in Figs. 4a and 4b, respectively. However, the convenient measure of the surface LDOS is the normalized tunneling conductance

ACCEPTED MANUSCRIPT

(dI/dV)/(I/V) [24], and for metallic or semiconducting surfaces the maxima observed in (dI/dV)/(I/V) characteristics can be often related to the existence of surface states [30] or defect states [31]. Thus, we will focus on (dI/dV)/(I/V) analysis in more detail (Fig. 4b). Curve #1 is representative for the straight part of the SiCNW and curve #2 is representative for the region of the bend. There are at least three important differences between these curves. The first is the shape which resembles "U" for curve #1 and "V" for curve #2. This change suggests that the LDOS below and above the Fermi level (E_F) is enhanced over the bend. The second is the shift of the global minimum from about 0 V (outside the bend) to –0.1 V (over the bend), and this in turn suggests the tendency to move E_F slightly towards the conduction band near the deformation of the SiCNW. The third observation is that the lowest LDOS value at E_F is non-zero for both curve #1 and curve #2, but over the bend (curve #2) the LDOS at E_F is higher than outside the bend (curve #1). All these facts suggest that the SICNW's surface is not homogenous and it is probably more metallic in the vicinity of the deformation.

It should be stressed that in the case of our measurement of the deformed SiCNW, the energy positions of LDOS peaks are slightly varying and depend on position of the STM tip over the scanned object which in turn can be ascribed to the local variation of the SiCNW's structure. For this reason, we have performed a statistical analysis of the energy distribution of LDOS maxima. Two rectangular regions are selected outside the bend (region I on the left side and region III on the right side, respectively; see Fig. 2b) and the region embracing the bend (region II, Fig. 2b). The area of the analysis is always the same and equals to 81×286 nm^2. To extract the statistical distribution of (dI/dV)/(I/V) maxima, we use the self-written software allowing the first order derivative calculation by applying the spline

ACCEPTED MANUSCRIPT

interpolation procedure and finding a local maximum for each point of each curve from a selected CITS region. Then, a histogram is constructed by counting the number of obtained maxima in the given energy range (bin size: 0.03 eV). In fact, we count the number of (dI/dV)/(I/V) maxima for each energy value (128 points) and for each curve (approximately 4200 curves in the area of analysis) and make a separate histogram for each region. In the Fig. 5a, the histograms corresponding to three different regions of the SiCNW are presented. In our opinion, the histograms on the left and on the right side (i.e. outside) of the bend, are relatively similar because they seem to show predominant existence of four maxima below the E_F (valence band) at around -0.2 eV, -0.4 eV, -0.6 eV and -0.8 eV. However, the maxima for region III seem to be better pronounced than the maxima for region I. This can be probably related to the lower roughness of the SiCNW of region III in comparison with region I. Although the maxima from regions I and III are distributed quite periodically, we suppose that they should rather not be attributed to the Coulomb blockade effect (CBE) which can appear in double barrier tunnelling system (tip-SiCNW and SiCNW-substrate) because: (i) the maxima appear only at negative voltages (CBE emerges typically at both negative and positive bias voltages [32]); (ii) the observed SiCNW is too large to exhibit CBE (good comparison can be made with much smaller single-walled carbon nanotubes where CBE was detectable [33]). The almost periodic order of peaks in region I and III is not reproduced over the bend (region II) where we can only see one pronounced maximum at around -0.3 eV and weakly pronounced features at -0.6÷-0.5 eV. It means that the LDOS close to the SiCNW's deformation is strongly affected by the existing defects and, as a result, the LDOS is inhomogeneous. This causes the variation of LDOS maxima over the bend and their appearance at many different positions in energy scale that results in a rather

ACCEPTED MANUSCRIPT

flat histogram. The characteristic maximum at -0.3 eV seems to be correlated with the deformation region as presented on the LDOS map in Fig. 5b. We can see that bright spots are located mostly over the bend which means that the deformation is probably related to the enhanced LDOS at -0.3 eV of the SiCNW's. We should admit that above E_F (conduction band) the number of counted maxima is a few times smaller than below E_F, so we have decided not to analyse these parts of histograms because of their lower statistical importance. Although there seems to be a difference between the histograms representing straight parts of SiCNW and the region of deformation, the exact interpretation of the observed peak positions is a point to debate. For the straight SiCNWs, we proposed three hypotheses to explain the origin of LDOS maxima: the disturbances of nitrogen-related donor band, the defects states assigned to the subsurface carbon enrichment, and the surface states attributed to the reconstruction process on the SiC nanowire surface (see also [21] and references therein). In this context we suppose that the change of SiCNW's electronic properties in the vicinity of a bend should be rather assigned to the specific chemical composition/stoichiometry and presumably local carbon-enrichment.

The recently reported experimental investigations of the influence of the defective regions on the SiCNWs' electronic structure suggest additional factors that should be taken into account [33]. The authors detected the inner potential bending in SiCNWs across the interface of the perfect crystal and the defective regions using electron holography and they also proposed the creation of a p-n junction in a SiCNW. Along with the authors, we think that not only the structure or stoichiometry fluctuations but also the segregation of impurities can be responsible for this local change of SiCNW's electronic structure. We suppose that in our case the most probable dopant is nitrogen which was detected in our samples using x-ray

Accepted Manuscript

ACCEPTED MANUSCRIPT

photoelectron spectroscopy (XPS) [22]. Because N can act as a donor in SiC material, it seems to be reasonable that structurally defective and porous parts of SiCNWs can be subject to contamination and local doping. We suppose that increased concentration of nitrogen close to the structural deformation can be responsible for the apparent LDOS fluctuations.

There is also another important factor which should be taken into account in the analysis of the CITS data which is related to the possible oxidation of the SiCNWs' surface. The existence of thin SiO_2 overlayer cannot be excluded in our case because the samples are prepared in ambient air atmosphere and are not cleaned under UHV conditions. Our previous XPS measurements also revealed noticeable amount of oxygen in SiCNWs' material [22]. As has been shown previously [34], the SiC/SiO2 interface on SiC monocrystallic surfaces introduces new electronic states that are ascribed to formation of sp^2-bonded carbon clusters, graphite-like clusters and oxide traps. It has also been proposed there that in the case of 3C-SiC surfaces especially the graphite-like defects can significantly alter the interface LDOS at energies close to the 3C-SiC conduction band edge. On the other hand, the sp^2-bonded carbon clusters can modify LDOS going from E_F towards the valence band edge. The STM/STS investigations performed on oxidized 6H-SiC (0001) [35] and 3C-SiC (001) [36] surfaces confirm that the formation of SiO_2 layer influences STS results. For instance, the (dI/dV)/(IV) curves in [36] exhibit the shift of the curves global minima (and also the valence band edge) towards the E_F along with local surface oxidation. In this context we suppose that the oxide overlayer can influence the surface electronic structure of SiCNWs, but in our case the situation seems to be even more complicated becasue: (i) we are dealing with a 1-D structure and not a monocrystalline surface, so the simple comparison between SiCNWs and 3C-SiC

ACCEPTED MANUSCRIPT

surfaces cannot be made, (ii) the SiCNWs' sidewalls can have various crystallographic orientation, (iii) one should take into account the influence of other contaminations (e.g. nitrogen) or non-stoichiometry (e.g. carbon enrichment) and their interference (e.g. the formation of silicon oxynitride [37]). Thus, we think that the presence of oxide layer can influence STS measurements both on straight and bended parts of SiCNWs. The changing of the thickness or the composition of oxide layer may be partially responsible for the local fluctuations of the (dI/dV)/(IV) spectra. Unfortunately, this influence cannot be unambiguously determined based on the STM/STS results only. Nevertheless, we think that the oxide insulating overlayer (if exists) must be rather thin (less than 1 nm) as it still allows stable STM measurements. Otherwise the tip would crash the sample because of the mechanical contact with the insulating layer. We claim that the full picture cannot be drawn here. Our new experiments are in progress to establish the SiCNWs cleaning procedure under UHV conditions and to determine the influence of different contaminations and their interferences on SiCNWs' surface electronic properties.

4. Summary

We investigated the morphology and the electronic structure of defected SiCNW produced via combustion synthesis. The STM images revealed the complicated structure of the bended SiCNW. The measurements performed in the CITS mode allowed us to correlate the surface topography with the accompanying I(V) and LDOS variations in the vicinity of the deformation region. The STS data showed the evolution of the I(V) characteristics from asymmetric shape towards symmetric shape. The evolution of LDOS exhibiting the enhanced values below E_F

ACCEPTED MANUSCRIPT

and shift of the global minimum towards conduction band were related to the possible metalicity of the deformation. The statistical analysis of the LDOS over the deformation revealed the predominant existence of the maximum at 0.3 eV below E_F. The behaviour of both I(V) and LDOS was ascribed to the inhomogeneous chemical composition of the defected SiCNW's region and probably to its partial surface graphitisation. The unintentional nitrogen doping was also considered as a reason for the metallic LDOS in the vicinity of the SiCNW's deformation. The formation of the thin oxide overlayer (SiO_2) is also taken into account to explain the fluctuations of the local electronic properties on the SiCNWs' surface.

Acknowledgements

This research was partly financed by European Regional Development Fund within the framework of Operational Programme Innovative Economy 2007-2013 (No. UDA-POIG.01.03.01-14-071/08-00). The work was supported by the UL Grant no. 505/697. The authors would like to acknowledge the software support of P. J. Kowalczyk.

Accepted Manuscript

ACCEPTED MANUSCRIPT

References

[1] S. Dimitrijev, Microel. Eng. 83 (2006) 123.

[2] C.I. Harris, S. Savage, A. Konstantinov, M. Bakowski, P. Ericsson, Appl. Surf. Sci. 184 (2001) 393.

[3] W.M. Zhou, F. Fang, Z.Y. Hou, L.J. Yan, Y.F. Zhang, IEEE El. Dev. Lett. 27 (2006) 463.

[4] J.Y. Fan, X.L. Wu, P.K. Chu, Prog. Mater. Sci. 51 (2006) 983

[5] C.N.R. Rao, F.L. Deepak, G. Gundiah, A. Govindaraj, Progress in Solid State Chemistry 31 (2003) 5.

[6] A. Huczko, M. Bystrzejewski, H. Lange, A. Fabianowska, S. Cudziło, A. Panas, M. Szala, J. Phys. Chem. B 109 (2005)16244.

[7] H. Kohno, H. Yoshida, Physica B 376–377 (2006) 890.

[8] S.Z. Deng, Z.S. Wu, J. Zhou, N.S. Xu, J. Chen, J. Chen, Chem. Phys. Lett. 364 (2002) 608.

[9] M.A. Makeev, D. Srivastava, M. Menon, Phys. Rev. B 74 (2006) 165303.

[10] D.N. McIlroy, A. Alkhateeb, D. Zhang, D.E. Aston, A.C. Marcy, M.G. Norton, J. Phys.: Condens. Matter 16 (2004) R415.

[11] W.M. Zhou, B. Yang, Z.X. Yang, F. Zhu, L.J.Yan, Y.F. Zhang, Appl. Surf. Sci. 252 (2006) 5143.

[12] F. Bechstedt, A. Fissel, J. Furthmüller, U. Grossner, A. Zywietz, J. Phys.: Condens. Matter 13 (2001) 9027.

[13] J.M. Lento, L. Torpo, T.E.M. Staab, R.M. Nieminen, J. Phys.: Condens. Matter 16 (2004) 1053.

Accepted Manuscript

ACCEPTED MANUSCRIPT

[14] A. Jorio, G. Dresselhaus, M.S. Dresselhaus, *Carbon Nanotubes: Advanced Topics in the Synthesis, Structure, Properties and Applications*, Springer Series in Topics in Applied Physics, vol. 111, Springer, Berlin, 2008.

[15] J.E. Lowther, J. Phys. C: Solid State Phys. 10 (1977) 2501.

[16] Y. Li, P.J. Lin-Chung, Phys. Rev. B 36 (1987) 1130.

[17] G. Cubiotti, Y. Kucherenko, A. Yaresko, A. Perlov, V. Antonov, J. Phys.: Condens. Matter 11 (1999) 2265.

[18] H. Iwata, U. Lindefelt, S. Öberg, P.R. Briddon, Phys. Rev. B 65 (2001) 033203.

[19] H. Matsuura, H. Nagasawa, K. Yagi, T. Kawahara, J. Appl. Phys. 96 (2004) 7346.

[20] A. Gali, Phys. Rev. B 73 (2006) 245415.

[21] A. Busiakiewicz, Z. Klusek, P.J. Kowalczyk, A. Huczko, S. Cudziło, P.K. Datta, W. Olejniczak, Surf. Sci. 602 (2008) 316.

[22] A. Busiakiewicz, A. Huczko, H. Lange, P.J. Kowalczyk, M. Rogala, W. Kozłowski, Z. Klusek, W. Olejniczak, K. Polański, S. Cudziło, Phys. Stat. Sol. (b) 245 (2008) 2094.

[23] R. Rurali, Phys. Rev. B 71 (2005) 205405.

[24] R. Feenstra, J. Stroscio, A. Fein, Surf. Sci. 181 (1987) 295.

[25] R. Feenstra, Phys. Rev. B 50 (1994) 4561.

[26] P. Kim, T.W. Odom, J. Huang, C.M. Lieber, Carbon 38 (2000) 1741.

[27] A. Busiakiewicz, Z. Klusek, A. Huczko, P.J. Kowalczyk, P. Dabrowski, W. Kozłowski, S. Cudziło, P.K. Datta, W. Olejniczak, Appl. Surf. Sci. 254 (2008) 4268.

[28] Z. Klusek, Z. Waqar, E.A. Denisov, T.N. Kompaniets, I.V. Makarenko, A.N. Titkov, A.S. Bhatti, Appl. Surf. Sci. 161 (2000) 508.

Accepted Manuscript

ACCEPTED MANUSCRIPT

[29] F. Gao, W.J. Weber, M. Posselt, V. Belko, Phys. Rev. B 69 (2004) 245205.

[30] V.A. Gasparov, M. Riehl-Chudoba, B. Schröter, W. Richter, Europhys. Lett. 51 (2000) 527.

[31] B. Stankiewicz, W. Kamiński, L. Jurczyszyn, Appl. Surf. Sci. 238 (2004) 36.

[32] H. Zhang, Y. Yasutake, Y. Shichibu, T. Teranishi, Y. Majima, Phys. Rev. B 72 (2005) 205441.

[33] T.W. Odom, J.-L. Huang, C.M. Lieber, J. Phys.: Condens. Matter 14 (2002) R145.

[34] V.V. Afanasev, M. Bassler, G. Pensl, M. Schulz, Phys. Stat. Sol. (a) 162 (1997)

[35] S. Nie, R.M. Feenstra, Mater. Sci. Forum 527-529 (2006) 1023.

[36] A. Mayne, F. Semond, G. Dujardin, P. Soukiassian, Phys. Rev. B 57 (1998) R15108.

[37] T. Shirasawa, K. Hayashi, S. Mizuno, S. Tanaka, K. Nakatsuji, F. Komori, H. Tochihara, Phys. Rev. Lett. 98 (2007) 136105.

Accepted Manuscript

ACCEPTED MANUSCRIPT

Figure Captions

Fig. 1. The SEM image (50 × 50 μm^2) showing the concentration, distribution and typical shapes of SiCNWs deposited on HOPG substrate (see text for details).

Fig. 2. (a) The topographic STM image (U_s=+1.0 V, I=0.1 nA) presenting the bend of the SiCNW. White arrows denote broken fragments of the nanowire that are clearly exposed. (b) The filtered topographic STM image (standard deviation filter) showing detailed structure of the bended SiCNW. Trenches running along the nanowire and complicated structure of the bend are visible. I, II and III denote the regions for further analysis and for the construction of histograms in Fig. 4a (see text for details).

Fig. 3. Comparison of I(V) traces for different parts of the defective SiCNW: region I outside the bend on the left side of the nanowire (denoted as "left", dashed line); region III outside the bend on the right side of the nanowire (denoted as "right", dash-dotted line); region II over the bend (denoted as "bend", solid line); and the region of the graphite substrate (denoted as "HOPG", dotted line).

Fig. 4. The representative (a) dI/dV and (b) corresponding (dI/dV)/(I/V) characteristics for the SiCNW's surface outside (curve #1, typical for regions I and III) and over the bend (curve #2, typical for region II).

Fig. 5. (a) Histograms representing the distribution of LDOS maxima over three rectangular regions: two outside the bend (regions I and III) and one over the bend (region II); (b) the LDOS distribution map in the vicinity of the SiCNW's bend recorded at the energy 0.3 eV below E_F.

Accepted Manuscript

ACCEPTED MANUSCRIPT

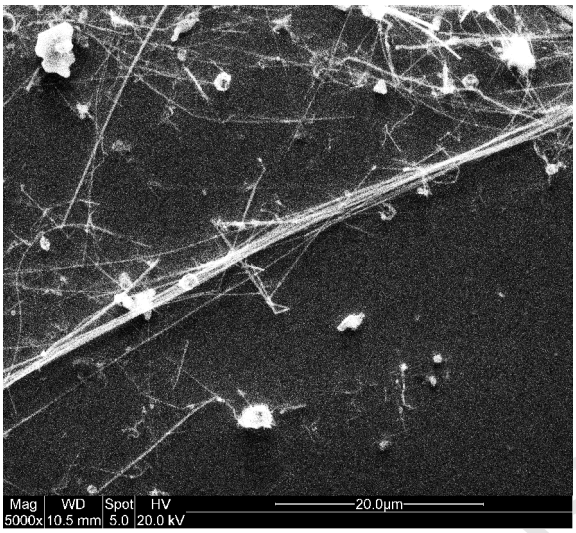


Figure 1

Accepted Manuscript

ACCEPTED MANUSCRIPT

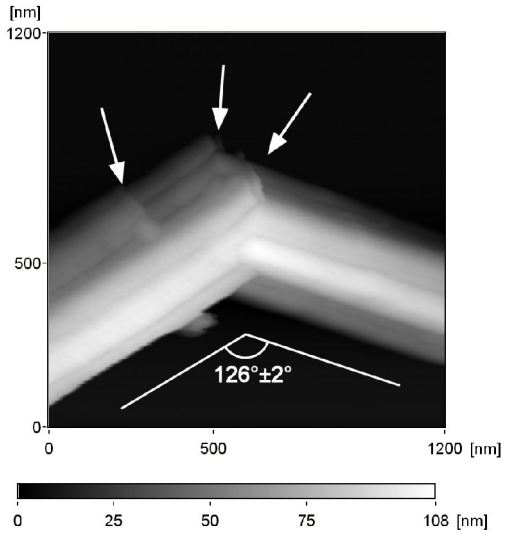


Figure 2a

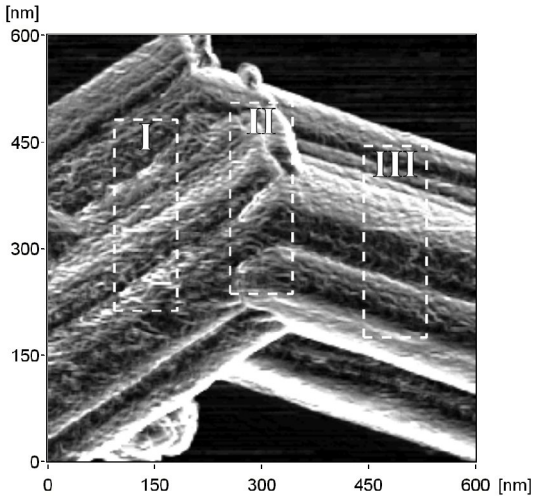


Figure 2b

ACCEPTED MANUSCRIPT

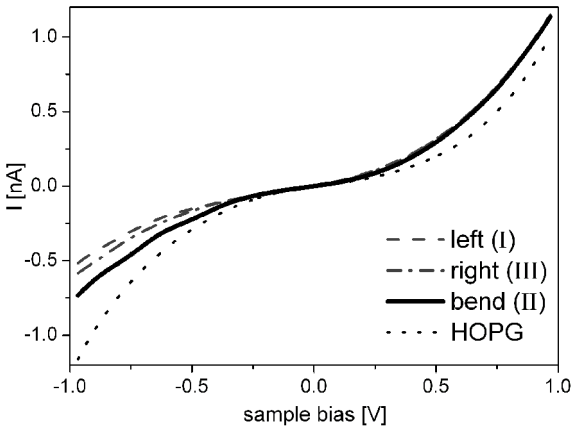


Figure 3

Accepted Manuscript

ACCEPTED MANUSCRIPT

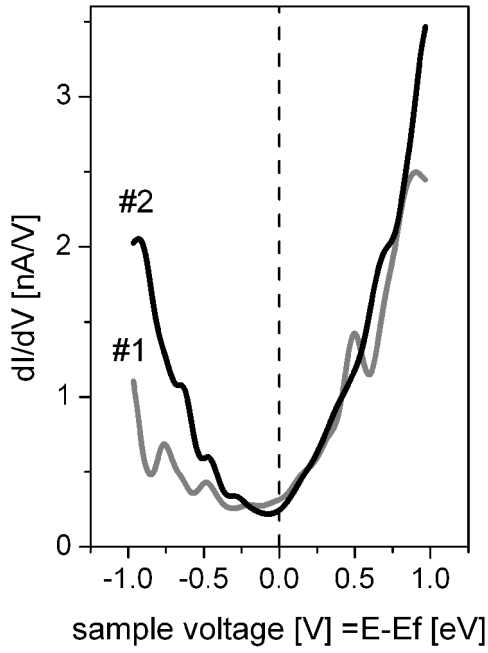


Figure 4a

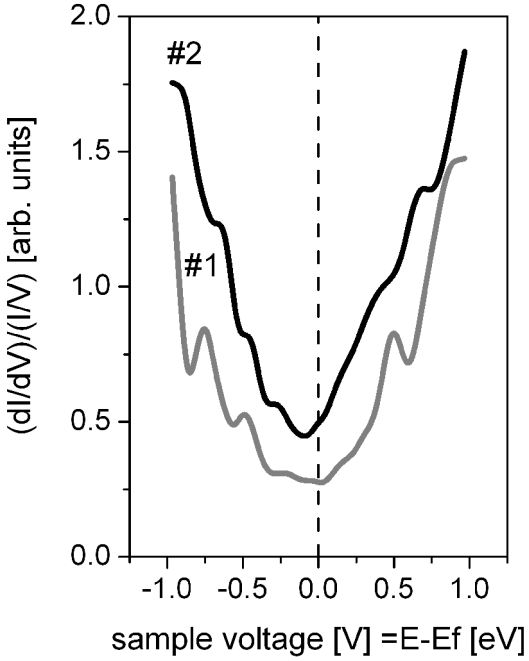


Figure 4b

ACCEPTED MANUSCRIPT

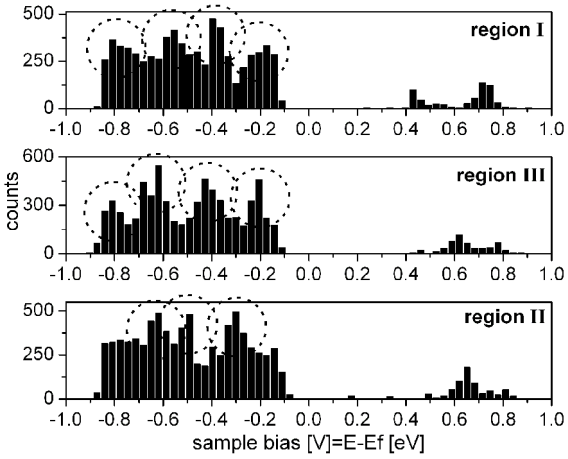


Figure 5a

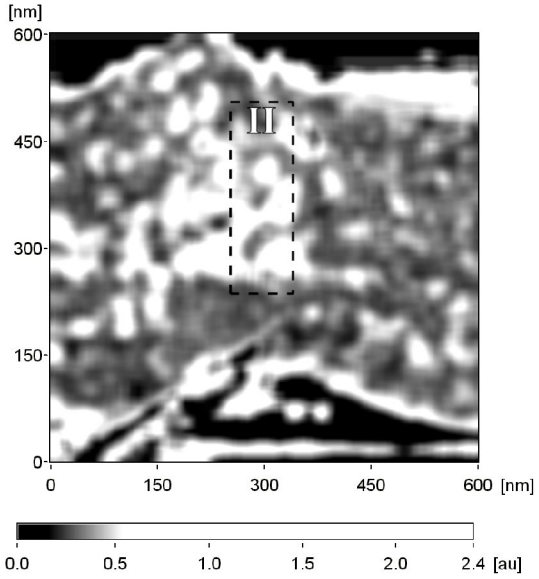


Figure 5b



https://dspace.org/

Defects of SiC nanowires studied by STM and STS

Busiakiewicz, Adam; Huczko, A.; Dudziak, Tomasz; Puchalski, M.; Kozlowski, W. ...

2010-05-01T00:00:00Z
Elsevier Science B.V., Amsterdam.
http://dx.doi.org/10.1016/j.apsusc.2010.01.102
A. Busiakiewicz, A. Huczko, T. Dudziak, M. Puchalski, W. Kozlowski, M. Cichomski, S. Cudzilo, Z. Klusek, W. Olejniczak, Defects of SiC nanowires studied by STM and STS, Applied Surface Science, Volume 256, Issue 15, 15 May 2010, Pages 4771-4776, Proceedings of the 4th International Workshop on Surface Physics 'Surfaces and Nanostructures'

Downloaded from a DSpace repository. https://dspace.org/